Nuclear Inst. and Methods in Physics Research B 463 (2020) 472–475

Contents lists available at ScienceDirect

Nuclear Inst. and Methods in Physics Research B

journal homepage: www.elsevier.com/locate/nimb

In-source laser spectroscopy of dysprosium isotopes at the ISOLDE-RILIS

K. Chrysalidis[a,b,*], A.E. Barzakh[c], R. Ahmed[d], A.N. Andreyev[e], J. Ballof[a,f], J.G. Cubiss[e], D.V. Fedorov[c], V.N. Fedosseev[a], L.M. Fraile[a,g], R.D. Harding[e], U. Köster[h], B.A. Marsh[a], C. Raison[e], J.P. Ramos[a], R.E. Rossel[a], S. Rothe[a], K. Wendt[b], S.G. Wilkins[a]

[a] CERN, CH-1211 Geneva, Switzerland
[b] Institut für Physik, Johannes Gutenberg-Universität, D-55099 Mainz, Germany
[c] Petersburg Nuclear Physics Institute (NRC Kurchatov Institute), RU-188300 Gatchina, Russia
[d] National Center for Physics, PAK-2141 Islamabad, Pakistan
[e] Department of Physics, University of York, UK-YO10 5DD York, United Kingdom
[f] Institut für Kernchemie, Johannes Gutenberg-Universität, D-55099 Mainz, Germany
[g] Grupo de Física Nuclear & IPARCOS, Universidad Complutense de Madrid, E-28040 Madrid, Spain
[h] Institut Laue-Langevin, F-38042 Grenoble, France

ARTICLE INFO

Keywords:
In-source laser spectroscopy
ISOLDE
RILIS
Dysprosium

ABSTRACT

A number of radiogenically produced dysprosium isotopes have been studied by in-source laser spectroscopy at ISOLDE using the Resonance Ionization Laser Ion Source (RILIS). Isotope shifts were measured relative to ^{152}Dy in the $4f^{10}6s^2\,{}^5I_8$ (gs) → $4f^{10}6s6p\,(8,1)^o_8$ (418.8 nm_{vac}) resonance transition. The electronic factor, *F*, and mass shift factor, *M*, were extracted and used for determining the changes in mean-squared charge radii for ^{145m}Dy and ^{147m}Dy for the first time.

1. Introduction

The Resonance Ionization Laser Ion Source (RILIS) is the most selective of all ion sources available at the ISOLDE radioactive beam facility [1]. The selectivity is an intrinsic property of the ionization mechanism, based on stepwise resonance excitation and ionization via element-specific atomic levels. The isotope production takes place inside a thick target, on which protons, provided by CERN's Proton Synchrotron Booster (PSB), impinge with an energy of 1.4 GeV. The reaction products are released from the target material and effuse via a transfer line into a resistively heated tubular cavity, where the atom-laser interaction takes place. The resulting ions are then extracted, accelerated up to 60 keV and mass separated by a dipole magnet according to their mass-to-charge ratio.

During so-called 'in-source laser spectroscopy', the RILIS lasers are used a to probe a specific spectroscopic transition of the ionization scheme of different isotopes of one element. By determining the isotope shift (IS) of a chosen transition, changes in the nuclear mean-squared charge radii can be deduced. For states with nonzero nuclear spin *I* which exhibit a sufficiently large hyperfine structure (HFS), the nuclear moments (spin, magnetic dipole and electric quadrupole moments) can be extracted. Additionally, if the HFS of different isomers can be resolved (due to different spins and magnetic moments), isomer-selective ionization is possible. The spectral resolution of in-source measurements is limited by Doppler-broadening of the spectral lines inside the ion source (which is typically heated to ≈ 2100 °C). There have been several experimental campaigns, in which this in-source spectroscopy has been successfully applied (e.g. [2]) or where isomer separation was provided for higher selectivity during nuclear spectroscopy experiments (e.g. [3]).

Here, we report on the first in-source spectroscopy study of dysprosium radioisotopes, demonstrating the suitability of this method for a future extended study of IS in the dysprosium isotopic chain.

2. Experimental setup

The experiment was performed using beam provided by target #655 (target with tantalum rolls from mixed 25 and 6 μm foils at 1950 °C with a tungsten surface ion source at 1985 °C). No stable supply of dysprosium was available initially, so that the optimization was performed on radiogenically produced ^{159}Dy. During the experiment, a proton current of 0.2 μA was used on target, providing a continuous supply of dysprosium.

The transition chosen for the spectroscopy leads from the $[Xe]4f^{10}6s^2\,{}^5I_8$ ground state to the $4f^{10}6s6p(8,1)^o_8$ excited state at 23877.74 cm^{-1} (≈ 418.8 nm) [4] (note: wavelengths given for vacuum).

* Corresponding author at: CERN, CH-1211 Geneva, Switzerland.
E-mail address: kchrysal@cern.ch (K. Chrysalidis).

https://doi.org/10.1016/j.nimb.2019.04.021
Received 14 January 2019; Received in revised form 26 March 2019; Accepted 10 April 2019
Available online 27 April 2019
0168-583X/ © 2019 The Authors. Published by Elsevier B.V. This is an open access article under the CC BY license (http://creativecommons.org/licenses/BY/4.0/).

A second laser, a non-tunable Nd:YVO_4 laser (2nd harmonic, 532 nm), results in efficient ionization of Dy from the $4f^{10}6s6p$, $J = 8$ excited level, despite the photon energy at 532 nm being below that required to reach the ionization continuum. The ionization efficiency saturates with an estimated 7 W of laser power in the ionization region (≈ 3 mm laser beam diameter). From this we conclude that the 532 nm light is coincidentally resonant with a second step transition to a high-lying level, from which a second 532 nm photon induces ionization via an auto-ionizing state. In the transition metals, the atomic level density, and the richness of the autoionizing spectrum, greatly increase the likelihood of such a coincidence in required transition wavelengths.

A newly developed narrow-linewidth intra-cavity frequency-doubled mode for the Ti:sapphire grating laser was applied for the first time, scanning across the 418.8 nm transition. It will be described in more detail in [5]. The wavelength was recorded with two High-Finesse/Angstrom WS7 wavelength meters installed in the RILIS laboratory. The wavemeters were calibrated before the measurements with a CW diode laser locked to the rubidium hyperfine structure. As the transition probability lies at $A = 1.26 \times 10^8\ s^{-1}$ [6], the power of the first-step laser beam had to be reduced significantly, to < 1 mW in order to avoid saturation.

For the cases of ^{148,149,165,158,159}Dy, the ISOLDE Faraday cups were used for ion beam detection, as the resonant ion rates were sufficiently high (> 1 pA). For ^{145,149,147}Dy the ISOLDE tape station gamma detector was utilized (for more details see [7]). An overview over the yields measured with the tape station β-counting is given in Table 1.

3. Results

In the case of ^{147}Dy, a long-lived isomeric state ($I_m = 11/2^-$ with $T_{1/2} = 55$ s) exists in addition to the ground state ($I_g = 1/2^+$ with $T_{1/2} = 67$ s). When monitoring the number of photoions in dependence of the first-step laser frequency by the intensity of the internal nuclear transition (678 keV, [12]) one obtains the optical spectrum of the pure high-spin isomer. Several γ-lines following the β-decay of ^{147g}Dy and ^{147m}Dy (101, 253, 365 keV [12]) were also present in the collected γ-spectra. Corresponding optical spectra are the mixture of that for metastable and ground state. The yield of ^{147m}Dy is estimated to be ∼ 5 times larger than the yield of ^{147g}Dy, following analysis of the γ-line intensities. As a result, it is impossible to estimate the IS of the ground state with reasonable accuracy.

For the case of ^{145}Dy ($I_m = 11/2^-$ with $T_{1/2} = 14$ s and $I_g = 1/2^+$ with $T_{1/2} = 6/$,s), only the γ-line resulting from the ^{145m}Dy β-decay at 639 keV was observed. The missing observation of other lines is attributed to the high background from the β-decay of the surface ionized isobars. Correspondingly, only results for the isomeric state were obtained.

The optical spectra are summarized in Fig. 1 and the IS are summarized in Table 2. Due to high background levels, stemming from the surface ionization of dysprosium and other isobaric (lanthanide) contaminants, the uncertainties of the IS are rather large (200–400 MHz). The signal-to-background ratio in case of e.g. ^{148}Dy is only 0.014. The same is true for the γ-spectra, where close lying, more intense γ-lines from isobaric contaminants dominate.

For extracting variations of the mean-squared charge radii $\delta\langle r^2\rangle$, results of the IS measurements with the 421.3 nm transitions from [13]

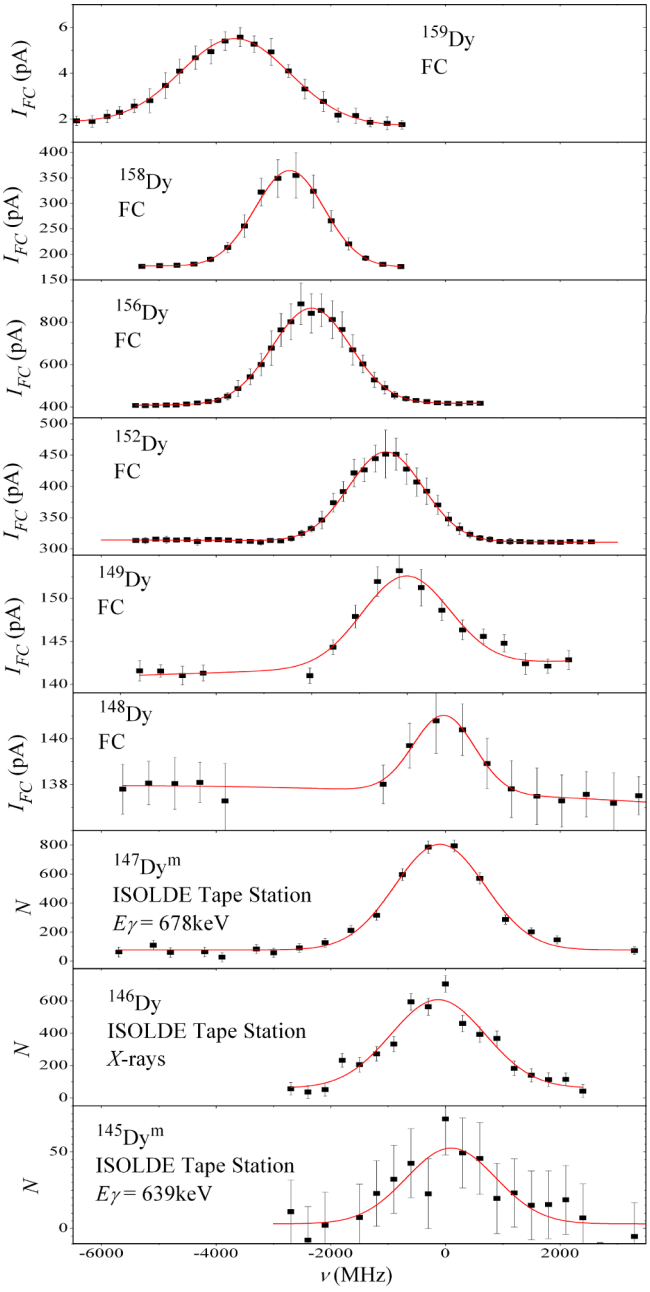

Fig. 1. Spectra for ^{159,158,156,152,149,148,147m,146,145m}Dy isotopes. For the odd-A dysprosium isotopes, the resolution was not high enough to resolve the HFS and therefore only the isotope shifts were extracted. The shift in center of gravity (CoG), introduced by the underlying HFS for these cases, was taken into account by estimating it with reasonable A and B HFS-constants: A- and B-constants ratios for the excited and ground states were taken from [9], for ^{159,148,147m}Dy the known Q and μ values [10] were used to calculate A and B constants by the standard scaling relation [11], μ (^{145m}Dy) and Q (^{145m}Dy) were set to be equal to the corresponding values for ^{147m}Dy with the same shell-model configuration ($\nu h_{11/2}$). The shift proved to be less than ∼ 40 MHz and was added to the uncertainties of the IS for the odd Dy isotopes.

Table 1
Extracted yields for different dysprosium isotopes with target #655. For ^{145,147}Dy it is not possible to give separate yields, as the ratio of the isomer production is not known. For ^{149}Dy the isomer contribution is assumed to be negligible due to the much shorter $T_{1/2}$. The accuracy of the measured yields can be estimated as a factor of two, taking into account the daughter activity contribution, isomer mixture and the possible contributions from the adjacent masses.

Dy mass	$T_{1/2}$	Yield [1/μC]	ABRABLA [8] in-target production
145(g/m)	14.5/6 s	1.3×10^5	1.9×10^9
146	29 s	2.1×10^6	3.5×10^9
147(g/m)	55/40 s	5.5×10^6	9.1×10^9
148	3.1 m	2.4×10^7	2.6×10^{10}
149	4.2 m	2.0×10^7	1.9×10^{10}
152	2.4 h	3.1×10^8	2.6×10^{10}
155	10.0 h	2.6×10^8	7.6×10^9

Table 2
Isotope shifts and changes in the mean-square charge radii for Dy isotopes. The errors result from the fitting procedure, described in Fig. 1.

A	$\delta\nu_{A,152}$ (MHz)	$\delta\langle r^2\rangle_{A,152}$ (fm^2)[a]	$\delta\langle r^2\rangle_{A,152}$ (fm^2)[b]
145 m	2270(430)	−0.63(12)	
146	1980(210)	−0.55(6)	−0.55(5)
147 m	1970(230)	−0.55(7)	
148	1970(120)	−0.55(3)	−0.53(5)
149	1560(280)	−0.43(8)	−0.41(4)
156	−2580(120)	0.72(3)	0.73(7)
158	−3380(100)	0.94(3)	0.94(9)
159	−3390(300)	0.94(8)	0.95(9)

[a] Present work.
[b] Reference [13].

were used for comparison. A 'standard' King-plot procedure (see e.g. [11]) is not possible, due to missing IS data for the light dysprosium isotopes (only $\delta\langle r^2\rangle$ are cited in [13,11]). A modified approach was used. Starting with the well-known relation that

$$\delta\nu_{A,A_0} = F\cdot\delta\langle r^2\rangle_{A,A_0} + M\cdot\frac{A-A_0}{A\cdot A_0}, \tag{1}$$

it follows that the modified IS

$$\sigma_\nu = \delta\nu_{A,A_0}\cdot\frac{A\cdot A_0}{A-A_0} \tag{2}$$

is linearly dependent on the modified $\delta\langle r^2\rangle$

$$\sigma_r = \delta\langle r^2\rangle_{A,A_0}\cdot\frac{A\cdot A_0}{A-A_0} \tag{3}$$

with the slope equal to the electronic factor F and the intercept equal to the mass-shift constant M:

$$\sigma_\nu = F\cdot\sigma_r + M \tag{4}$$

The nuclear masses A and A_0 used in the calculations by Eqs. (1)–(3) were taken from [14].

As shown in Fig. 2, all newly measured modified IS for the 418.8 nm transition, as well as the previously measured $\sigma_{418.8\,\mathrm{nm}}$ for $A, A_0 = 164, 160$ [15] over modified $\delta\langle r^2\rangle$ lie on a straight line, testifying to the consistency of the newly obtained data. From this plot, the electronic factor F and mass-shift factor M were determined to be $F_{418.8\,\mathrm{nm}} = -3580(110)$ MHz fm^{-2} and $M_{418.8\,\mathrm{nm}} = -60(360)$ GHz amu (note, that the uncertainty of the F and M factors for the previously

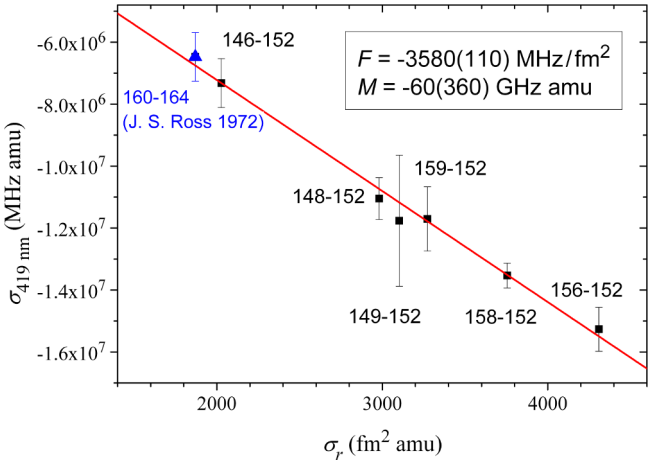

Fig. 2. Modified King-plot for extraction of the F and M factors for the 418.8 nm transition. IS data for this transition are from the present work (black squares) and from Ref. [15] (blue triangle). (For interpretation of the references to colour in this figure legend, the reader is referred to the web version of this article.)

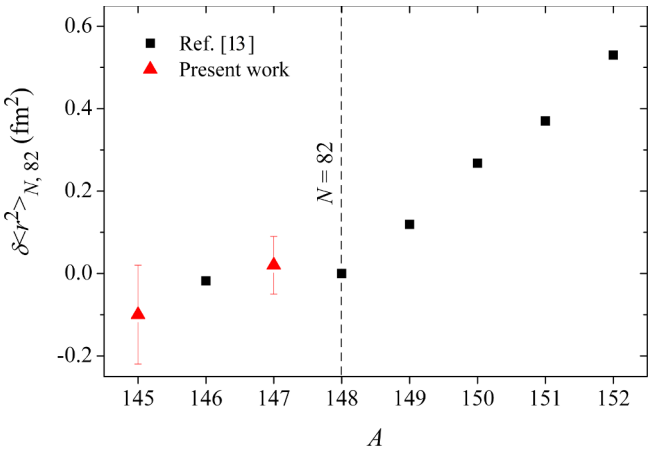

Fig. 3. Changes in $\delta\langle r^2\rangle$ in the vicinity of the $N = 82$ shell closure with the newly obtained values for the high-spin isomers of ^{145m,147m}Dy and data taken from [13].

studied 421-nm transition are not taken into account. These values were cited in [11] without uncertainties). With the derived F and M factors, changes in $\delta\langle r^2\rangle$ for the high-spin isomers in ^{147,145}Dy were derived for the first time (see Table 2).

Fig. 3 shows the newly obtained values for $\delta\langle r^2\rangle^{145^m,148}$ and $\delta\langle r^2\rangle^{147^m,148}$ together with the data taken from [13] for $N = 78, 83-86$ relative to ^{148}Dy. The shell effect in the $\delta\langle r^2\rangle$ (kink at $N = 82$) is evident for odd- and even-N isotopes. It was found previously that there is a marked isomer shift between $1/2^+$ ground states and $11/2^-$ isomers in $_{62}$Sm and $_{64}$Gd nuclei at $N < 82$ [16,17]. This isomer shift leads to the disappearance of the odd-even staggering (OES) in $\delta\langle r^2\rangle$ of the $11/2^-$ isomers. The results obtained in the present work for $11/2^-$ dysprosium isomers do not contradict this observation, although no definite conclusion can be inferred due to the large experimental uncertainties.

4. Outlook

In order to better investigate the disappearance of normal OES in the vicinity of $N = 82$ for the high-spin isomers in dysprosium, expected to be influenced by the $\nu h_{11/2}$-state, further studies with dedicated beam time are necessary. A better resolution of the γ-spectra and detection efficiency, using the ISOLDE Decay Station (IDS), would help to separate the ground from isomeric state. The relative uncertainties could be additionally reduced by using the transition to the $4f^{10}6s6p$, $J = 9$ state at 23736.61 cm^{-1} ($\approx$ 421.3 nm). This transition has been shown to have an isotope-shift sensitivity twice the size of the 418.8 nm transition [11]. As seen in Table 2 and Fig. 1, at the signal to background ratio larger than ~ 1 and sufficient statistics the uncertainty of the IS determination can be reduced to 100 MHz (^{158}Dy) and lower (taking into account reduction of the uncertainty also for CoG measurement for the reference isotope). This accuracy is expected to be sufficient to investigate the evolution of OES (see results for similar 11/2-state in Sm [16]). However, more accurate results may be achieved with better resolution which would enable reliable analysis of the odd Dy isotope HFS.

It is estimated that dysprosium isotopes down to around $A = 141$ are accessible for IS measurements by the in-source spectroscopy method, provided sufficient suppression of isobaric background is achieved (e.g. with the Laser Ion Source and Trap (LIST) [18]). It is worth to note that dysprosium isotopes with $A < 146$ have noticeable delayed proton branching and photo-ion current monitoring by delayed protons detection might give more favorable background conditions. Near this point, a strong onset of deformation is expected which would be reflected in the IS values.

Acknowledgments

This work has received funding from the European Union's Horizon 2020 research and innovation program under grant agreement No 654002 and from the Russian Foundation for Basic Research (RFBR) under research project No 19-02-00005.

References

[1] V. Fedosseev, et al., J. Phys. G 44 (2017) 084006 .
[2] B.A. Marsh, et al., Nat. Phys. 14 (2018) 1163–1167.
[3] M. Piersa, et al., Phys. Rev. C 99 (2019) 024303 .
[4] NIST Atomic Level Database (last extracted 01.12.2018).
[5] K. Chrysalidis, et al., Technical review of Ti:sapphire laser development within the scope of JRA RESIST, In preparation (2019).
[6] NIST Atomic Lines Database (last extracted 01.12.2018).
[7] R. Catherall, et al., J. Phys. G 44 (2017) 094002 .
[8] A. Kelic, et al., 2009. arXiv:0906.4193.
[9] N. Leefer, et al., Opt. Lett. 34 (2009) 2548.
[10] N. Stone, At. Data Nucl. Data Tables 90 (2005) 75–176.
[11] E.W. Otten, Treatise on heavy ion science, Nuclei Far From Stab. 8 (1989) 517–638.
[12] Brookhaven National Nuclear Data Center (extracted 26.10.2018).
[13] I. Angeli, K. Marinova, At. Data Nuclear Data Tables 99 (2013) 69–95.
[14] M. Wang, et al., Chin. Phys. C 41 (2017) 030003 .
[15] J.S. Ross, J. Opt. Soc. Am. 62 (1972) 548–554.
[16] V.S. Letokhov, et al., J. Phys. G 18 (1992) 1177.
[17] A.E. Barzakh, et al., Phys. Rev. C 72 (2005) 017301 .
[18] D. Fink, et al., NIMB 344 (2015) 83–95.